Accepted Manuscript

Influence of oxide matrix on electron transport in $(FeCoZr)_x(Al_2O_3)_{1-x}$ nanocomposite films

Ivan A. Svito, Alexander K. Fedotov, Anis Saad, Pawel Zukowski, Tomasz N. Koltunowicz

PII: S0925-8388(17)30063-4

DOI: 10.1016/j.jallcom.2017.01.043

Reference: JALCOM 40410

To appear in: *Journal of Alloys and Compounds*

Received Date: 6 December 2016

Revised Date: 3 January 2017

Accepted Date: 4 January 2017

Please cite this article as: I.A. Svito, A.K. Fedotov, A. Saad, P. Zukowski, T.N. Koltunowicz, Influence of oxide matrix on electron transport in $(FeCoZr)_x(Al_2O_3)_{1-x}$ nanocomposite films, *Journal of Alloys and Compounds* (2017), doi: 10.1016/j.jallcom.2017.01.043.

Influence of oxide matrix on electron transport in $(FeCoZr)_x(Al_2O_3)_{1-x}$ nanocomposite films

Ivan A. Svito[1], Alexander K. Fedotov[1], Anis Saad[2], Pawel Zukowski[3], Tomasz N. Koltunowicz[3,*]

[1] Belarusian State University, 4, Nezalezhnastsi Av., Minsk 220030, Belarus

[2] Al-Balqa Applied University, PO Box 4545, Amman 11953, Jordan

[3] Lublin University of Technology, 38d, Nadbystrzycka Str., 20-618 Lublin, Poland

Abstract

Electron transport in $(Fe_{0.45}Co_{0.45}Zr_{0.10})_x(Al_2O_3)_{1-x}$ granular nanocomposites (NCs) produced by the ion-beam sputtering of compound target was studied in the temperature range of 2–300 K. Conductivity of the films synthesized in the inert (Ar) atmosphere is determined below percolation threshold by the thermally activated electron tunneling over metallic granules at low temperatures and replaced by the Mott variable range hopping (VRH) with increasing temperature. Introduction of oxygen to the sputtering chamber suppresses VRH leading to retention of the thermally activated tunneling in the whole studied temperature range for the metallic phase atomic concentrations up to $x = 0.62$. The model of thermally activated tunneling over metallic granules gives an excellent agreement with experimental data when alumina matrix permittivity is considered as increasing with concentration of the metallic phase fraction in the films, which is due to increase in number of localized electronic states. The established influence of the sputtering atmosphere on the electron transport in nanocomposites is explained by reduction of concentration of the defects in matrix when oxygen is added to the sputtering atmosphere.

Keywords: nanocomposite; oxide matrix; electron transport; thermally activated tunneling; ~~variable range hopping;~~ defects; permittivity

[*] Corresponding author. Tel: +48 81 5384713. E-mail: t.koltunowicz@pollub.pl (Tomasz N. Koltunowicz)

1 Introduction

The priorities in the development of science and technology is the creation and manufacture of novel materials. An important area of research in nanomaterials and nanotechnology is the surface engineering with nanostructured surfaces. This is the case of protective coatings in which nanocrystalline phases are embedded in an amorphous matrix [1-3].

Due to a small size (a few nanometers) of metallic particles randomly distributed in dielectric matrix, nanogranular metal-insulator composites reveal a number of important fundamental effects and interesting properties: hopping electron transport, spin-dependent tunneling magnetoresistance, superparamagnetic state of granules, giant Hall effect, etc. [4-10]. In particular, an interest in nanostructured films based on the ferromagnetic Fe-Co alloys is determined by prospects of their practical use as a magnetic head for information recording and read-out [11, 12], development of protective shields against electromagnetic radiation [13], magnetic field sensors, etc.

The structural, magnetic, magnetoresistive and other properties of the metal-dielectric $(FeCoZr)_x(Al_2O_3)_{1-x}$ nanocomposites produced by the ion-beam sputtering were investigated earlier [10, 14-19]. It was established by the TEM and XRD analyses that in such nanocomposites with concentration of metallic phase corresponding to the dielectric side of the metal-insulator transition (MIT), nanosized metallic nanoparticles formed by the FeCo alloy are randomly distributed in the Al_2O_3 amorphous matrix [15]. In works [14, 20], peculiarities of magnetic and electron transport properties of nanocomposites were explained taking into account formation of the „core-shell" structure with metallic granules covered by oxide shells in the case of addition of oxygen to the sputtering atmosphere. At the same time, influence of the oxide matrix state (first of all, concentration of defects) on electron transport in nanocomposites has not been yet taken into account, although matrix defectiveness can be of the crucial importance in the case of hopping electron transport. Just these circumstances have determined the goal of the presented research.

2. Experimental

$(Fe_{0.45}Co_{0.45}Zr_{0.10})_x(Al_2O_3)_{1-x}$ granular nanocomposite films were synthesized by the ion-beam sputtering of compound target in pure argon (p_{Ar}= 6.0×10^{-2} Pa) or mixed Ar+O_2 (partial pressures p_{Ar}=6.0×10^{-2} Pa, p_{O2}=4.3×10^{-3} Pa) atmospheres onto water-cooled glass-ceramic substrates. Detailed description of the synthesis procedure can be found in [21]. These two types of nanocomposites will be designated below as NC-Ar and NC-(Ar+O_2), respectively. The film thickness was equal to 3–6 μm according to the cross-section SEM experiments. Atomic concentration of metallic phase x in the films was determined by the EDX analysis and was varied from 0.31 to 0.64. Additionally, $Fe_{0.45}Co_{0.45}Zr_{0.10}$ pure metallic films were investigated as the reference samples.

Temperature dependences of conductivity were studied using a HFMS system (Cryogenic Limited, London), which allows setting the sample temperature in the range from 2 to 300 K with an accuracy better than 0.05 K. The samples of 2×7 mm^2 in size were provided by the ultrasonically soldered indium electric probes. DC conductivity measurements were realized using a Keithley 6430 Source-Meter and a Keithley 2182A nanovoltmeter. AC conductivity was measured at room temperature with Agilent E4980A and Agilent E4285A LCR-meters at the frequencies of 2 and 30 MHz with a probe voltage magnitude of 40 mV and using a standard correction procedure.

3. Results and Discussions

Our experiments have demonstrated that the shape of temperature dependence of electrical conductivity σ(T) changes significantly with increasing metallic phase concentration x for the composites synthesized in the Ar atmosphere (Fig. 1a). Conductivity of the films with high concentrations of metallic phase decreases with increasing temperature demonstrating a rather weak power-like σ(T) dependence, which is characteristic for metal-insulator composites above the percolation threshold x_c, i.e. on the metallic side of MIT. For the nanocomposites with $x < 0.56$, conductivity increases with temperature indicating prevailing of an activation-like carrier transport. For the intermediate range of metallic phase concentrations ($0.56 < x < 0.64$), a superposition of these

two ultimate cases of σ(*T*) behavior is observed (Fig. 1a). Note that in the concentration range of $0.48 < x < 0.52$, the temperature dependences of conductivity can be linearized in the $\sigma \sim \log(T)$ coordinates for a wide temperature range (Fig. 1a), which could be attributed to the tunneling conductivity with a large electron localization length and is inherent to materials with composition close to MIT [22-24].

For the nanocomposites synthesized in the $Ar+O_2$ atmosphere (Fig. 1b), the activation type of σ(*T*) dependences (peculiar for the metal-insulator composites on the dielectric side of MIT) is observed for the whole studied range of the metallic phase concentration ($0.31 < x < 0.64$), and no change in $d\sigma/dT$ sign occurs.

As is seen from Fig. 1, analysis of σ(*T*) dependences does not allow correct determining the percolation threshold x_c giving rise to necessity to develop alternative methods for obtaining x_c value. As is seen from Fig. 2, we can present x_c basing on the analysis of phase shift between AC current and voltage depending on the metallic phase concentration *x*. Since any conductor has an inductance, impedance of the composites with metallic phase concentration $x \geq x_c$ has an inductive-like type due to formation of continuous conductive cluster between two electric probes. On the other hand, if $x < x_c$ and metallic particles are separated by oxide interlayers, impedance is capacitive-like [25, 26].

As is seen from Fig. 2, for the NC-Ar nanocomposites, impedance changes from capacitive-like to inductive-like with increasing *x* and indicating formation of the continuous conductive cluster at $x_c \approx 0.49$. This allows attributing this concentration as corresponding to the MIT position. On the contrary, in the case of the NC-($Ar+O_2$) nanocomposites, a capacitive-like impedance is conserved in the whole concentration range. The observed difference in θ(*x*) dependences for two types of the studied nanocomposites correlates well with changes in their σ(*T*) behavior with increasing *x* and indicates the lack of insulator-metal transition in the NC-($Ar+O_2$) films even at the largest *x* values studied. The observed dielectric-like properties of the NC-($Ar+O_2$) composites with a large content of metallic phase can be explained by formation of thin oxide shells around metallic granules due to a presence of oxygen in the sputtering chamber [14, 20].

Analysis of results presented in Fig. 1 has demonstrated that σ(T) dependences for the nanocomposites on the dielectric side of MIT are described well by the Mott-like law:

$$\sigma(T) = \sigma_0 \exp[-\left(\frac{T_0}{T}\right)^n], \quad (1)$$

where n equals 0.5 or 0.25 (see below), and T_0 is a parameter, which characterizes activation energy of electron tunneling through barriers.

For the NC-Ar nanocomposites with $x \leq x_c \approx 0.49$ (which corresponds to the volume fraction less than 0.24), there is a concentration dependent crossover temperature $T_c(x)$, which decreases monotonically from 130 to 60 K when x is increasing. An exponent in the equation (1) equals to $n = 0.5$ at $T < T_c$, whereas $n = 0.25$ at $T > T_c$ (Fig. 3).

For the nanocomposites synthesized in the Ar+O_2 atmosphere, the temperature dependences of conductivity are linearized in the $\ln(\sigma) \sim (T_0/T)^{0.5}$ coordinates at $x < 0.62$ in the whole temperature range (Fig. 3), and only composites with $x > 0.62$ demonstrate a crossover to $n = 0.25$ at $T > 200$ K.

The $\ln(\sigma) \sim (T_0/T)^{0.5}$ law is usually explained by the Coulomb gap in the density of localized electronic states (DOS) in accordance with the Efros-Shklovskii variable range hopping (VRH) law [27]. However, influence of the Coulomb gap on electron transport can appear only at low temperatures (as a rule, below 10 K) when a thermal energy is less than the gap width. We believe that the observed experimental results and, in particular, the $\ln(\sigma) \sim (T_0/T)^{0.5}$ law can be explained by the model of thermally activated electron tunneling between the metallic granules with some scattering of their sizes [28]. Use of this model is reasonable because size dispersion can reach 30 % for the nanocomposites produced by the ion-beam sputtering according to the previous studies [29, 30].

As is known, the exponent $n = 0.25$ in Eq. (1) can be attributed to the Mott VRH transport over the localized states [31]. These localized states in the alumina matrix can exist due to the following reasons. Firstly, amorphous matrix has a great number of structural defects such as uncoordinated Al atoms, as well as Fe and Co atoms, which do not belong to the metallic granules [30, 32, 33]. Secondly, in the case of ion-beam synthesis of nanocomposites in the Ar atmosphere, atomic composition of the matrix is deviated from stoichiometric toward oxygen deficiency as a rule [34].

This is due to the fact that part of oxygen atoms is knocked-out from the alumina part of target and carried away by a gas flow, as well as due to the presence of zirconium, which acts as a reducer [35]. The formed oxygen vacancies in alumina matrix play a role of localization centers [35, 36].

Existence of the above-mentioned structural defects in the alumina matrix gives rise to appearance of additional levels in the energy gap of alumina (Fig. 4), over which electron hopping can be realized [36, 37]. Since every electron jump is accompanied by emission or absorption of phonon, the cooling is accompanied with the decrease in a number of energetically acceptable states for electron hops leading to an increase of the jump length.

Thus, the VRH electron transport dominates until the jump length becomes equal to a mean distance between the nanogranules. Subsequent temperature decrease leads to the crossover of conductivity mechanism, when thermally activated electron tunneling becomes more energetically favorable. In this case, decrease of crossover temperature T_c with increasing metallic phase concentration correlates with the decrease of intergranular distance and increase of density of localized states in the matrix.

Figure 5 presents the parameter T_0 in Eq. (1) determined using linearization of temperature dependences of conductivity in the $\ln(\sigma) - (T_0/T)^{0.5}$ coordinates depending on the metallic phase concentration in the studied composites. As is seen from Fig. 5, T_0 decreases with increasing concentration of metallic phase. Especially fast fall of T_0 is observed in the NC-Ar films, when x is approaching the MIT value.

In the framework of the above-mentioned model of thermally activated electron tunneling between the metallic granules, the characteristic temperature T_0 in Eq. (1) is described by the expression [28]:

$$T_0 = \frac{e^2}{k_B \varepsilon a_0} \cdot \left(\frac{a_0}{\lambda}\right)^{3/2} \cdot \left[x_V^{-1/2} \cdot \left(1 - \frac{x_V}{x_{V_c}}\right)^{1/3}\right], \qquad (2)$$

where $\lambda = h/\sqrt{2mU_{ab}}$ is the decay length of the electron wave function in dielectric matrix, U_{ab} is the height of the intergranular tunnel barrier, m is the electron mass, ε is the dielectric permittivity of

matrix, a_0 is the average size of the metallic granules, and x_V is the volume fraction of the metallic component in nanocomposite (calculated under the assumption that all Fe and Co atoms are in the metallic (non-oxidized) state).

The following parameters were used for the estimation of T_0: U_{ab} = 3.5 eV (calculated as the difference between FeCo work function and alumina electron affinity); the average size of metallic granules a_0 was set as monotonically growing from 2 to 7 nm with increasing metallic phase concentration according to the previous TEM, XRD and magnetization studies [14, 15].

Dependence of static matrix permittivity ε on concentration of metallic phase in the composites (Fig. 6) has been estimated from Eq. (3). Position of MIT for the NC-(Ar+O_2) nanocomposites at higher concentration of the metallic phase ($x_c \approx 0.72$ corresponding to the volume fraction of 0.59) in comparison to the NC-Ar nanocomposites confirms the partial oxidation of a metallic component during NC deposition. Thereby, there is some uncertainty in determination of the volume fraction of the non-oxidized metallic component. However, this factor can not influence significantly on the x_V/x_{Vc} ratio in Eq. (2).

As is seen from Fig. 6, the matrix permittivity for the NC-Ar nanocomposites increases by appr. one order of magnitude when approaching MIT. Similar behavior was observed in a number of papers [38, 39]. From a physical point of view, the observed growth of permittivity can be related to the increase in concentration of point defects (for example, metallic atoms and vacancies) distributed in the amorphized alumina matrix during sputtering procedure and their contribution to the electric field screening.

Estimation of the density of localized states N_0 in alumina matrix was carried out in the hydrogen-like approximation using the following expression for permittivity [40]:

$$\varepsilon(N_0) = 1 + \frac{3(\varepsilon_r - 1)\beta_m + 3(\varepsilon_r - 1 + \beta_m)\alpha_0 N_0}{3\beta_m - (\varepsilon_r - 1 + \beta_m)\alpha_0 N_0}, \qquad (3)$$

where β_m is the parameter accounting a lattice symmetry and equal to 3 for a cubic lattice, as well as for amorphous materials, $\alpha_0 = 18\pi r^3$ is the polarizability of neutral hydrogen-like donor, $r = e^2/8\pi\varepsilon_r\varepsilon_0 I_d$ is the Bohr radius of the localized electron with the ionization energy I_d , ε_r is the permittivity close to

unity in our case due to comparability of the Bohr radius and lattice parameter. The used approximation of neutral centers is reasonable because conductivity is determined at $T < T_c$ mainly by the electron tunneling between metallic granules, whereas electron hopping over localized states is negligible indicating their neutral charge state.

As is seen from Fig. 7, the density of localized states increases with metallic phase concentration, being about half times higher for the NC-Ar samples as compared with NC-($Ar+O_2$) ones at close x values.

At the first glance, it could seem strange that defect concentration increases with decreasing dielectric component fraction. However, this effect can be naturally explained by elevation of heat conductivity of the composites with increasing x due to a large difference in heat conductivities of amorphous matrix (1.6–2 $W \times m^{-1} K^{-1}$) [41] and metallic alloy (80 $W \times m^{-1} K^{-1}$). High heat conductivity of nanocomposites with a large fraction of metallic phase leads to more fast energy loss by condensed atoms and, hence, loss of their difusibility in the growing film during ion-beam synthesis. This statement is supported by results of the Mossbauer spectroscopy, which demonstrate an increase of number of Fe^{2+} ions with increasing x [17]. Moreover, as it was above mentioned, the elevation of metallic phase fraction in the nanocomposites increases the number of Zr atoms, which are oxidized easily giving rise to the increase in concentration of oxygen-deficient defects in the matrix.

Therefore, the observed difference in electron transport properties for the NC-Ar and NC-($Ar+O_2$) nanocomposites can be explained by the fact that addition of oxygen to the sputtering atmosphere leads to reduction of the oxygen-deficient centers concentration in the films studied.

As was mentioned above, for the NC-Ar nanocomposites with $x < x_c$, the Mott VRH over localized states is observed at $T > T_c$ (Fig. 3). According to the Mott model [31], the $\ln(\sigma) \sim (T_0^M/T)^{0.25}$ law takes place for disordered systems. Plotting of experimental dependences for the temperature range $T > T_c$ in the form proposed by Kirkpatrick [42] enabled one to estimate the electron localization radius values in the nanocomposites on the dielectric side of MIT according to equation

$$a = \left[0.0217\left(\frac{4\cdot E_1^2 e^6}{9\cdot\pi\hbar^4 d s^5\cdot\varepsilon_M{}^2}\right)\cdot\left(\frac{1}{8.99\cdot10^{11}\cdot\sigma_0}\right)\right]^{1/3} \text{(cm)}, \quad (4)$$

and estimations of DOS at the Fermi level by equation

$$N(E_f) = \frac{60}{\pi k T_0 a^3} \ (\text{eV}^{-1}\text{cm}^{-3}), \quad (5)$$

where E_1 = 10 eV is the deformation potential of the alumina matrix, d = 3.55 g/cm^3 is the density of amorphous alumina, $s \approx 6.7\times10^5$ cm/s is the speed of sound [43], $\varepsilon_m \approx 17$ (Fig. 6) is the permittivity of the alumina matrix, e is the electron charge, $\hbar$ is the reduced Planck constant, k is the Boltzmann constant, and σ_0 is defined by the following relations:

$$\sigma_0 = 0.0217\left(\frac{C}{a}\right), \quad (6)$$

$$C = \left(\frac{E_1^2}{\pi d s^5 \hbar^4}\right)\cdot\left(\frac{2e^3}{3\varepsilon_m}\right)^2. \quad (7)$$

According to the calculation, electron localization radius at the dielectric side of MIT in NC-Ar composites is close to $a \approx 0.6$ nm for low metallic phase concentrations ($x < 0.34$), when the presence of metallic granules in the composites does not influence remarkably on their conductivity. Electron DOS at the Fermi level has been estimated as appr. 8×10^{20} cm^{-3}eV^{-1} for low values of metallic phase concentrations (0.30–0.34).

Conclusions

The performed investigation of electron transport in the $(Fe_{0.45}Co_{0.45}Zr_{0.10})_x(Al_2O_3)_{1-x}$ granular nanocomposites produced by the ion-beam sputtering of compound target in neutral (Ar) and oxygen-containing atmosphere in vacuum chamber enables one to draw the following conclusions:

1. Conductivity of the studied nanocomposites synthesized in the inert (argon) atmosphere below the percolation threshold is described well at low temperatures $T < T_c$ by the model of thermally activated tunneling over metallic granules with some size distribution. Crossover to the Mott variable range hopping takes place with the approaching T_c.

2. In nanocomposites synthesized with addition of oxygen into the sputtering chamber, the thermally activated intergranular tunneling of electrons is observed in the entire studied temperature range (2–300 K).
3. The observed difference in electron transport properties for the NC-Ar and NC-(Ar+O_2) nanocomposites (in particular, disappearance of the Mott variable range hopping in the case of nanocomposites synthesized in the oxygen-containing atmosphere) can be explained by the fact that addition of oxygen to the sputtering atmosphere leads to reduction of the oxygen-deficient centers concentration in the alumina matrix of the films studied.
4. The matrix permittivity for the NC-Ar nanocomposites increases by appr. one order of magnitude when approaching MIT that can be related to the growth in concentration of point defects (like, metallic atoms and vacancies) distributed in the amorphized alumina matrix during sputtering procedure and their contribution to the electric field screening.

Acknowledgements

Helpful discussions with N.A. Poklonski, E.A. Streltsov and A.V. Mazanik are acknowledged. This work was partly supported by the statute tasks of the Lublin University of Technology, at the Faculty of Electrical Engineering and Computer Science, 8620/E-361/S/2016 (S-28/E/2016), entitled "*Researches of electrical, magnetic, thermal and mechanical properties of modern electrotechnical and electronic materials, including nanomaterials and electrical devices and their components, in order to determination of suitability for use in electrical engineering and to increase the efficiency of energy management*".

References

[1] A.D. Pogrebnjak, I.V. Yakushchenko, O.V. Bondar, V.M. Beresnev, K. Oyoshi, O.M. Ivasishin, H. Amekura, Y. Takeda, M. Opielak, C. Kozak Irradiation resistance, microstructure and

mechanical properties of nanostructured (TiZrHfVNbTa)N coatings, Journal of Alloys and Compounds, 679 (2016), 155-163.

[2] A. Shypylenko, A.V. Pshyk, B. Grzeskowiak, K. Medjanik, B. Peplinska, K. Oyoshi, A. Pogrebnjak, S. Jurga, E. Coy, Effect of ion implantation on the physical and mechanical properties of Ti-Si-N multifunctional coatings for biomedical applications, Materials and Design, 110 (2016), 821-829.

[3] V. Ivashchenko, S. Veprek, A. Pogrebnjak, B. Postolnyi, First-principles quantum molecular dynamics study of TixZr 1-xN(111)/SiNy heterostructures and comparison with experimental results, Science and Technology of Advanced Materials, 15 (2) (2014), Article number 025007

[4] Y. Omata, H. Sakakima, Thermal stability of soft magnetic properties of Co-(Nb,Ta)-(Zr,Hf) films with high saturation magnetization, IEEE T. Magn. 23 (1987) 1005–1008.

[5] J.C. Denardin, M. Knobel, X.X. Zhang, A.B. Pakhomov, Giant Hall effect in superparamagnetic granular films, J. Magn. Magn. Mater. 262 (2003) 15-22.

[6] S. Mitani, Y. Shintani, S. Ohnuma, Giant magnetoresistance and Hall effect in Fe-based metal-oxide granular thin films, J. Magn. Soc. Jpn. 21 (1997) 465–468.

[7] P. Sheng, B. Abeles, Y. Arie, Hopping Conductivity in Granular Metals, Phys. Rev. Lett. 31, (1973) 44–47.

[8] S. Honda, T. Okada, M. Nawate, M. Tokumoto, Tunneling giant magnetoresistance in heterogeneous Fe-SiO_2 granular films, Phys. Rev. B., B56. (1997) 14566–14573.

[9] H. Fujimori, S. Mitani, S. Ohnuma, Tunnel-type GMR in metal-nonmetal granular alloy thin films, Mater. Sci. Eng. 31 (1997) 219–223.

[10] A.M. Saad, V.A. Kalaev, J.A. Fedotova, K.A. Sitnikov, A.V. Sitnikov, Yu.E. Kalinin, A.K. Fedotov, I.A. Svito, Strukture and magnetic properties of nanogranular composites CoFeZr – alumina, Rev. Adv. Mater. Sci 15 (2007) 208–214.

[11] M. Yu, Y. Liu, A. Moser, D. Weller, D. J. Sellmyer, Nanocomposite CoPt:C films for extremely high-density recording, Appl. Phys. Lett. 75, (1999) 3992–3994.

[12] A.V. Kimel, R.V. Pisarev, A.A. Rzhevskii, Y.E. Kalinin, A.V. Sitnikov, O.V. Stognei, F. Bentivegna and T. Rasing: Magnetooptical study of granular silicon oxide films with embedded CoNbTa ferromagnetic particles, Phys. Solid State, 45 (2003) 283–286.

[13] J.C.A. Huang, C.Y. Hsu, Complex capacitance spectroscopy as a probe for oxidation process of AlOx – based magnetic tunnel junctions, Appl. Phys. Lett. 85(24) (2004) 5947–5949.

[14] J. Fedotova, J. Przewoznik, Cz. Kapusta, M. Milosavljevicr, J.V. Kasiuk, J. Zukrowski, M. Sikora, A.A. Maximenko, D. Szepietowska, K.P. Homewood, Magnetoresistance in FeCoZr–Al_2O_3 nanocomposite films containing ‘metal core–oxide shell’ nanogranules, Phys. D Appl. Phys. 44 (2011) 495001–1–495001–12.

[15] I. Svito, J.A. Fedotova, M. Milosavljevic, P. Zhukowski, T.N. Koltunowicz, A. Saad, K. Kierczynski, A.K. Fedotov, Influence of sputtering atmosphere on hopping conductance in granularnanocomposite $(FeCoZr)_x(Al_2O_3)_{1-x}$ films, J. Alloy. Compd. 615 1 (2014) S344–S347.

[16] A.M. Saad, A.V. Mazanik, Yu.E. Kalinin, J.A. Fedotova, A.K. Fedotov, S. Wrotek, A.V. Sitnikov, I.A. Svito, Structure and electrical properties of CoFeZr-aluminium oxide nanocomposite films, Rev. Adv. Mater. Sci. 8 (2004) 152–157.

[17] J. Fedotova, J.Kalinin, A. Fedotov, A. Sitnikov, I. Svito, A. Zalesskij, The effect of the sputtering process ambient on the magnetic state and phase composition of the film nanocomposites $(Fe_{0.45}Co_{0.45}Zr_{0.10})_x(Al_2O_3)_{1-x}$, Hyperfine Interact. 165 (2005) 127–134.

[18] T.N. Kołtunowicz, P. Zukowski, J. Sidorenko, V. Bayev, J.A. Fedotova, M. Opielak, A. Marczuk: Ferromagnetic resonance spectroscopy of CoFeZr-Al2O3 granular films containing “FeCo core – oxide shell” nanoparticles, Journal of Magnetism and Magnetic Materials 421 (2017), 98–102.

[19] P. Zhukowski, J. Sidorenko, T.N. Kołtunowicz, J.A. Fedotova, A.V. Larkin: Magnetic properties of nanocomposites (CoFeZr)x(Al2O3)1-x, Przeglad Elektrotechniczny 86 (7) (2010) 296–298.

[20] J. Fedotova, J. Kasiuk, J. Przewoznik, Cz. Kapusta, I. Svito, Yu. Kalinin, A. Sitnikov, Effect of oxide shells on the magnetic and magnetotransport characteristics of oxidized FeCoZr nanogranules in Al_2O_3, J. Alloy. Compd. 509 (2011) 9869–9875.

[21] Yu.E. Kalinin, A.N. Remizov, and A.V. Sitnikov, Bulletin of Voronezh State Technical University: Material Science N113 (2003) 43–49.

[22] M.C. Chan, A.B. Pakhomov, Z.-Q. Zhang, Numerical study of conductance distribution in granular metal films, J. Appl. Phys. 87 (2000) 1584–1586.

[23] I. S. Beloborodov, K. B. Efetov, A.V. Lopatin, V. M. Vinokur, Transport Properties of Granular Metals at Low Temperatures. Phys. Rev. Lett. 91(24) (2003) 246801–4.

[24] I.S. Beloborodov, A.V. Lopatin, V.M. Vinokur, K.B. Efetov, Granular electronic systems, Rev.Mod. Phys. 79 (2007) 469–518.

[25] H. Bakkali, M. Dominguez, X. Batlle, A. Labarta, Universality of the electrical transport in granular metals, Sci. Rep. 6 (2016) 29676–8.

[26] F.C. Fonseca, R. Muccillo, Impedance spectroscopy analysis of percolation in (yttria-stabilized zirconia)-yttria ceramic composites, Solid State Ionics 166 (2004) 157–165.

[27] A.L. Efros, B.I. Shklovski, Conduction of nanostructured metall – insulator, Phys. Stat. Solid. B. 76 (1976) 475–490.

[28] E.Z. Meilikhov, Thermally activated conductivity and current-voltage characteristic of dielectric phase in granular metals, J. Exp. Theor. Phys. 88 (4) (1999) 819–825.

[29] K. Yakushiji, S. Mitani, K.Takanashi, J-G. Ha, H. Fujimori, Composition dependence of particle size distribution and giant magnetoresistance in Co-Al-O granular films, J. Magn. Magn. Mater. 212 (2000) 75–81.

[30] M. Ohnuma, K. Hono, H. Onodera, J.S. Pedersen, S. Mitani H. Fujimori, Distribution of Co Particles in Co-Al-O Granular Thin Films, Journal of Metastable and Nanocrystalline Materials V1 (1999) 171–176.

[31] N.F. Mott, E.A. Devis, Electron Processes in Noncrystalline Materials, Clarendon Press, Oxford (1979).

[32] E.Z. Kurmaev, D.A. Zatsepin, S.O. Cholakh, B. Schmidt, Y. Harada, T. Tokushima, H. Osawa, S. Shin, T. TakeuchiIron, Nanoparticles in amorphous SiO_2: X-ray emission and absorption spectra , Phys. Solid State 47 (2005) 754–757.

[33] M. Ohnuma, K. Hono, E. Abe, H. Onodera, S. Mitani, H. Fujimori, Microstructure of Co-Al-O granular thin films, J. Appl. Phys. 82 N.11 (1997) 5646 – 5652.

[34] O.V. Stognei, A.V. Sitnikov, Yu.E. Kalinin, S.F. Avdeev, M.N. Kopytin, Isotropic positive magnetoresistance in Co-Al_2O_n nanocomposites, Phys. Solid State 49 (2007) 164–170.

[35] T.V. Perevalov, O.E. Tereshenko, V.A. Gritsenko, V.A. Pustovarov , A.P. Yelisseyev, Chanjin Park, Jeong Hee Han, Choongman Lee, Oxygen Deficiency Defects in Amorphous Al_2O_3, J. Appl. Phys. 108 (2010) 013501–4.

[36] T.V. Perevalov, A.V. Shaposhnikov, V.A. Gritsenko, Electronic structure of bulk and defect α- and γ-Al_2O_3, Microelectronic Engineering. 86 (2009) 1915–1917.

[37] B.D. Evans, G.J. Pogatshnik and Y. Chen, Optical properties of lattice defects in α-Al_2O_3, Nucl. Instr. Meth. 91 (1994) 258–262.

[38] M. Lee, J. G. Massey, V. L. Nguyen, and B. I. Shklovskii, Coulomb gap in a doped semiconductor near the metal-insulator transition: Tunneling experiment and scaling ansatz, Phys. Rev. B 60 (1999) 1582–1591.

[39] T. G. Castner, N. K. Lee, H. S. Tan, L. Moberly, O. Symko, The low-frequency, low-temperature dielectric behavior of *n*-type germanium below the insulator-metal transition, J. Low Temp. Phys. 38 (1980) 447–473.

[40] N.A. Poklonski, S.A. Vyrko, A.G. Zabrodskii, Electrostatic models of insulator-metal and metal-insulator concentration phase transitions in Ge and Si crystals doped by hydrogen-like impurities, Phys. Solid State 46 (2004) 1101–1106.

[41] I. Stark, M. Stordeur, F. Syrowatka, Thermal conductivity of thin amorphous alumina films, Thin Solid Films 226-1 (1993) 185–190. doi: 10.1016/0040-6090(93)90227-G.

[42] K. Yasuda, A. Yoshida and T. Arizumi, The effects of anniling on Motts parameterrs for hopping conducthion in amorfous Ge, Phys. Stat. Sol. (a) 41 (1977) K181–K184.

[43] C. Rossignol, B. Perrin, and B. Bonello, Elastic properties of ultrathin permalloy/alumina multilayer films using picosecond ultrasonics and Brillouin light scattering, Phys. Rev. B 70 (2004) 094102–12.

Figure captions

Fig. 1. Temperature dependences of DC conductivity in the σ – log(*T*) coordinates for the $(FeCoZr)_x(Al_2O_3)_{1-x}$ nanocomposites synthesized in the Ar (*a*) and Ar+O_2 (*b*) atmospheres.

Fig. 2. Concentration dependences of phase shift angle θ between AC current and voltage for the $(FeCoZr)_x(Al_2O_3)_{1-x}$ nanocomposites synthesized in the Ar (left) and Ar+O_2 (right) atmospheres.

Fig. 3. Temperature dependences of conductivity for the NC-Ar (*a*) and NC-(Ar+O_2) (*b*) nanocomposites in the $\log(\sigma) - T^{-0.25}$ and $\log(\sigma) - T^{-0.5}$ coordinates for the samples with $x = 0.33$ (*1*), $x = 0.48$ (*2*), $x = 0.33$ (*3*), and $x = 0.64$ (*4*).

Fig. 4. Band diagram of $(FeCoZr)_x(Al_2O_3)_{1-x}$ nanocomposite.

Fig. 5. Concentration dependences of parameter T_0 in Eq. (1) for the NC-Ar and NC-(Ar+O_2) nanocomposites.

Fig. 6. Matrix permittivity *vs.* metallic phase concentration estimated using Eq. (3).

Fig. 7. Concentration of hydrogen-like defects in alumina matrix depending on the concentration of metallic phase *x* in the studied nanocomposites. Circles correspond to the values calculated according to Eq. (3); lines are given for convenience.

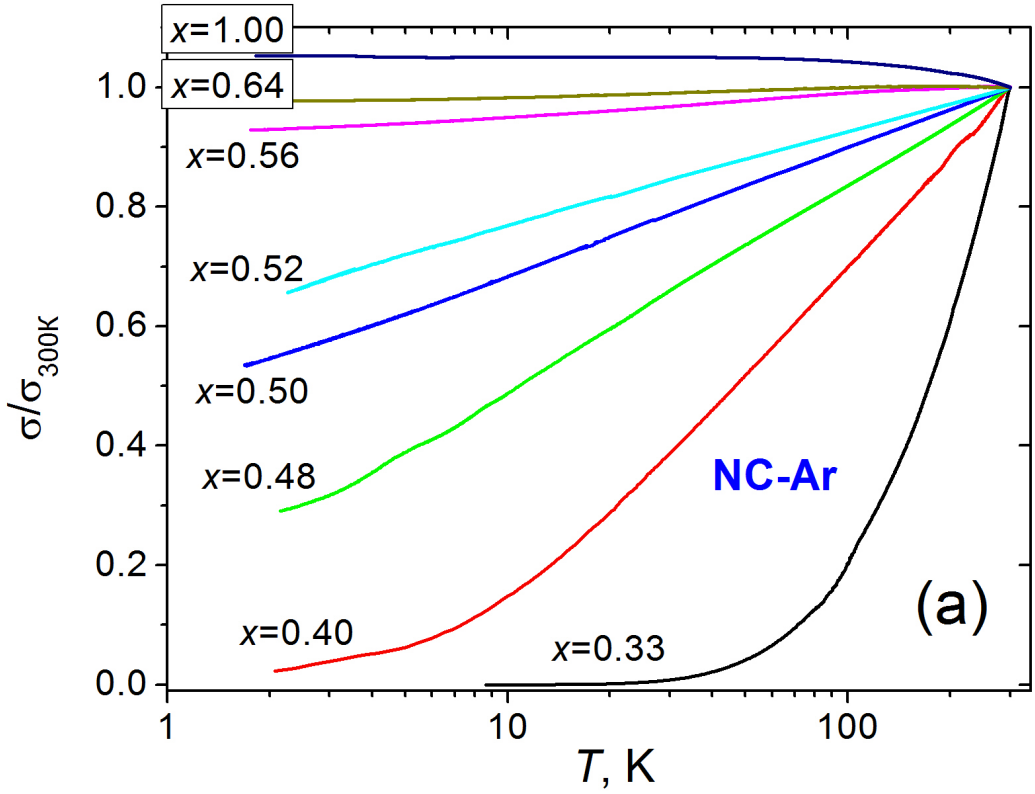

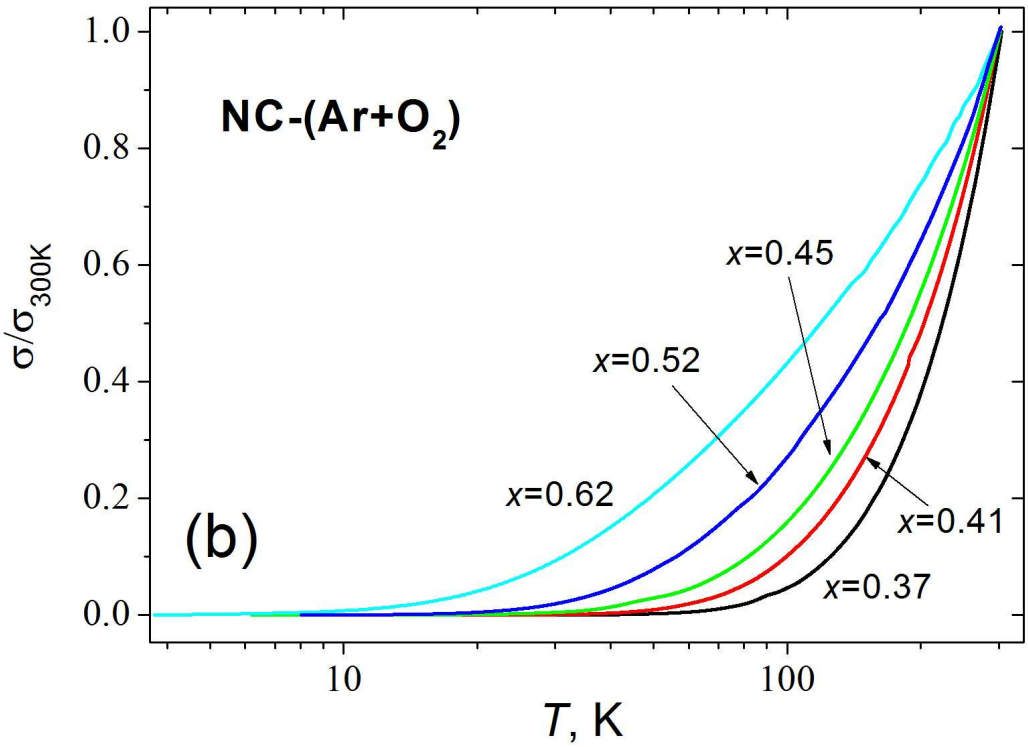

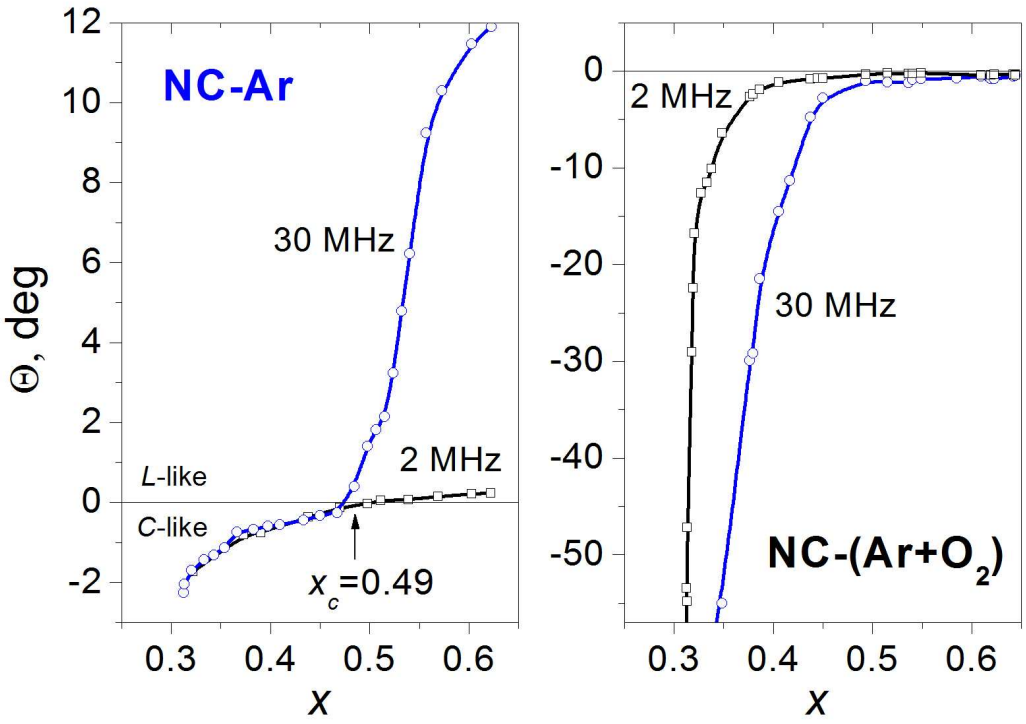

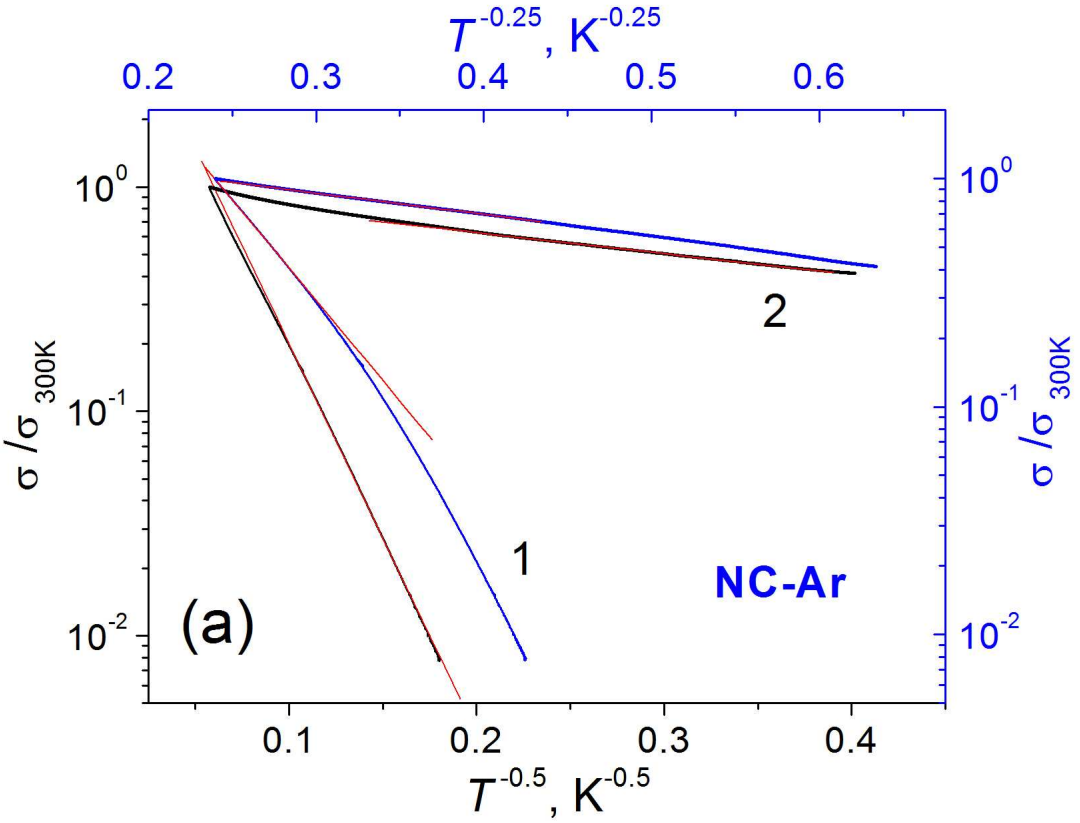

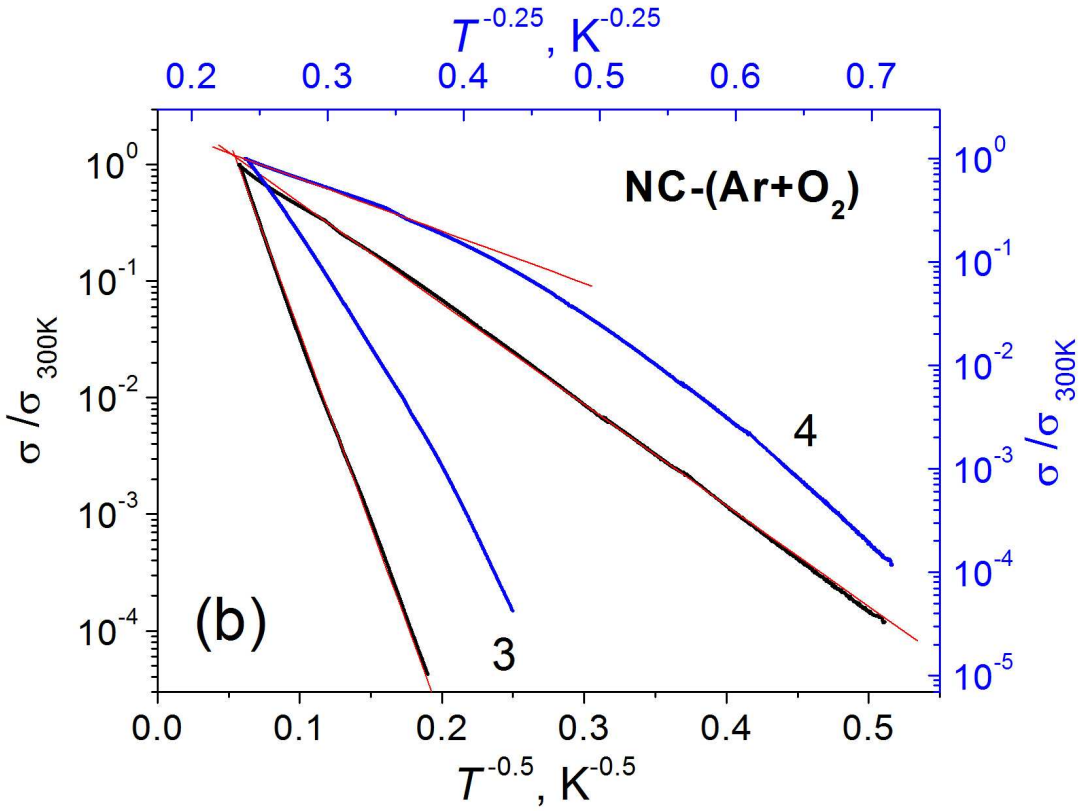

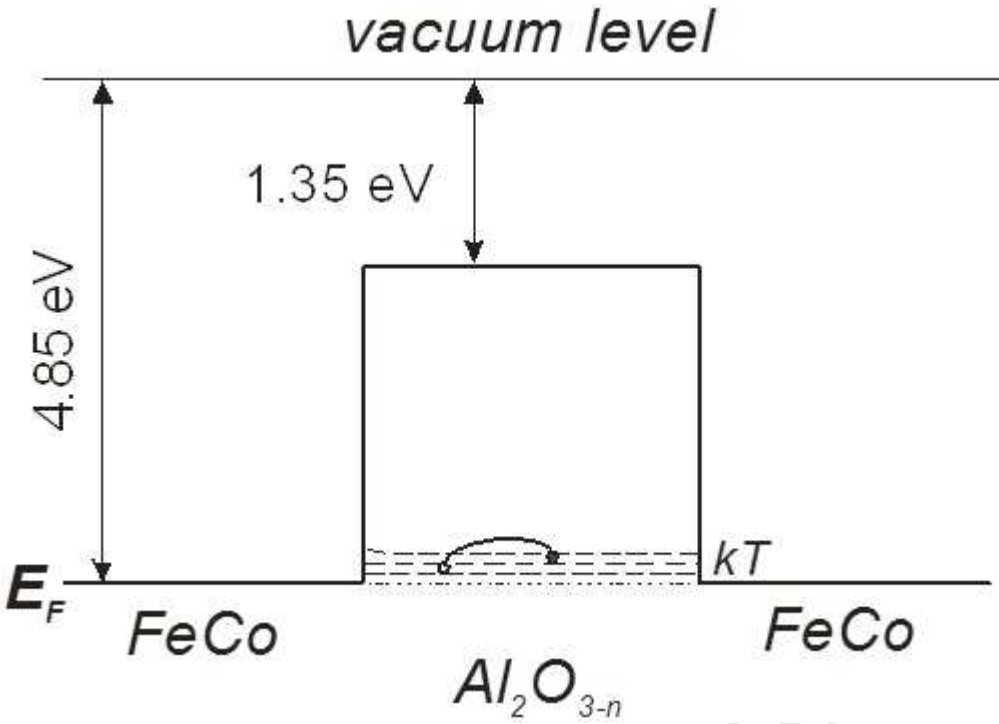

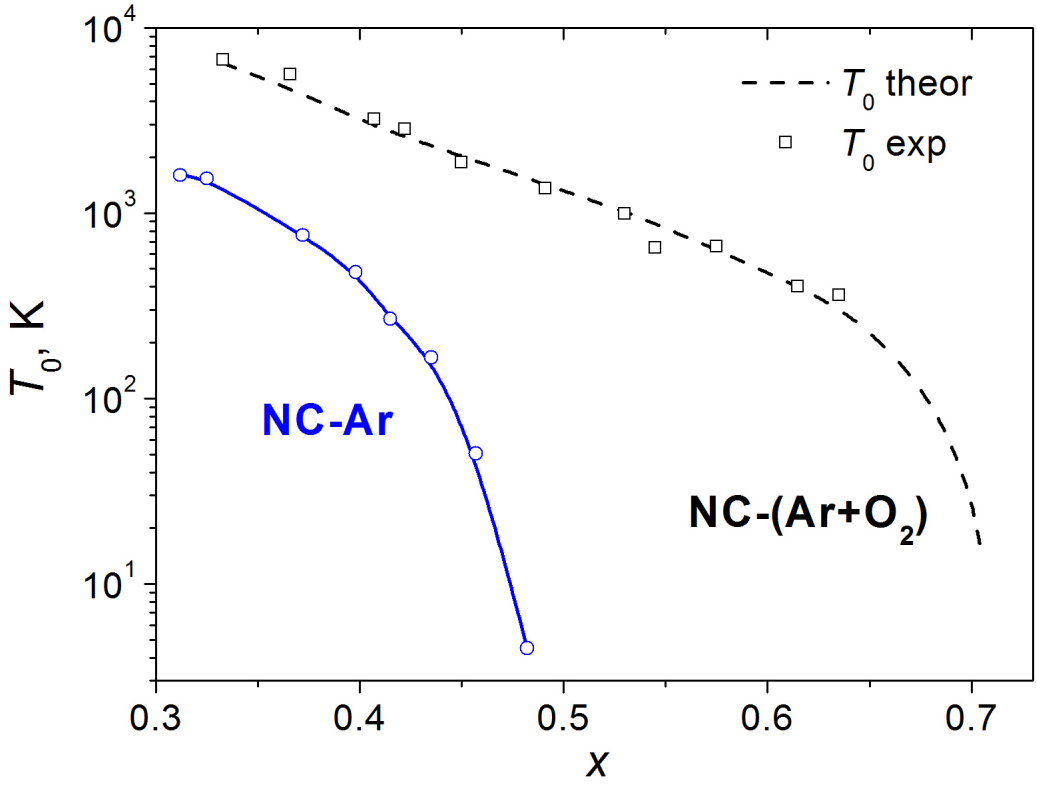

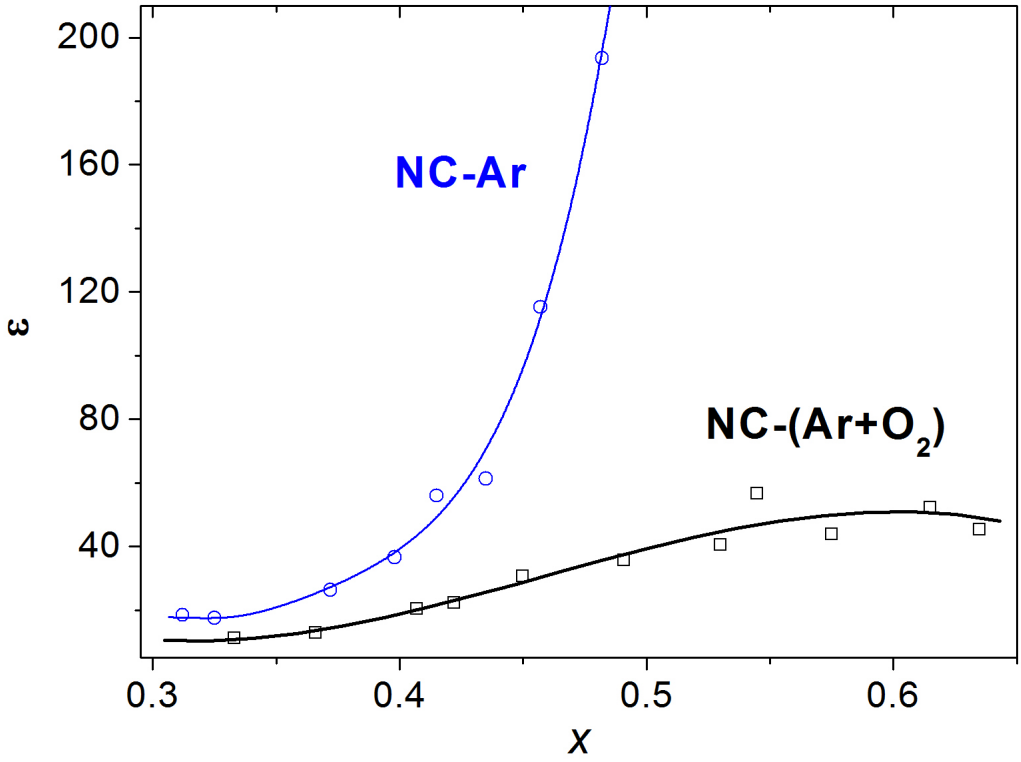

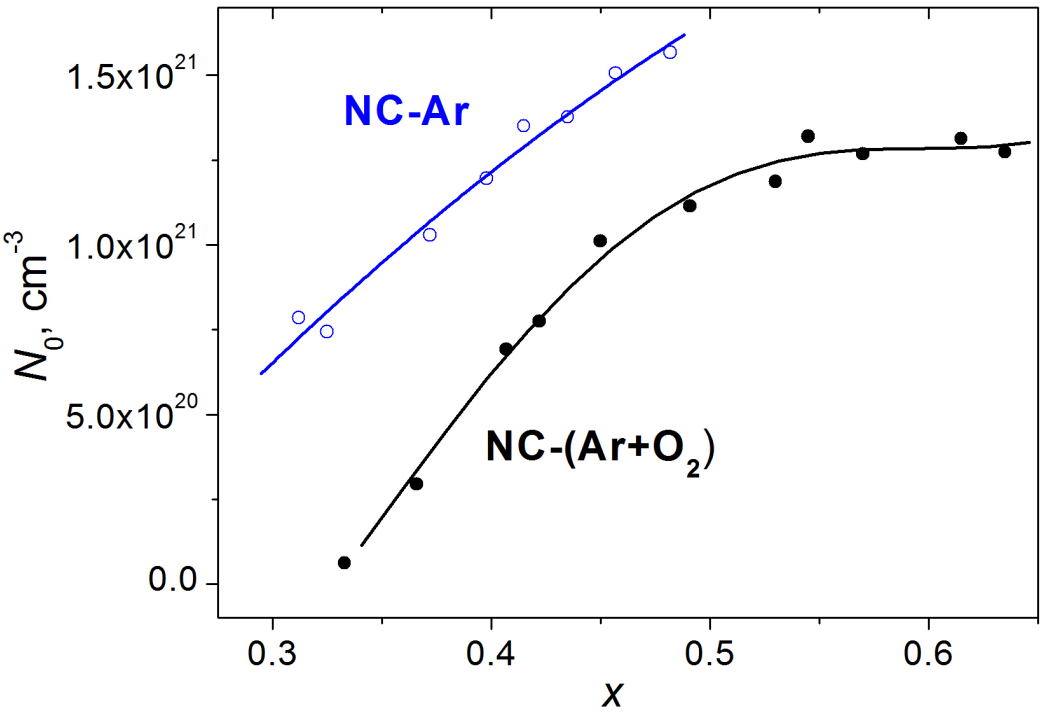

Highlights for paper

"Influence of oxide matrix on electron transport in $(FeCoZr)_x(Al_2O_3)_{1-x}$ nanocomposite films"

- Electron transport in nanocomposites produced by ion-beam sputtering was studied

- Addition of oxygen to sputtering atmosphere suppresses Mott hopping conductivity

- This effect is determined by oxygen-induced reduction of alumina matrix defectiveness